SOIL STRESS ANALYSIS AT DIFFERENT DEPTHS AFTER AGRICULTURAL VEHICLE OPERATION
/
农业车辆作业后不同深度的土壤应力分析

Jun GUO[1)]; Enhui SUN*[1)]; Yue YANG[1)]; Jun LU[1)]
[1)] School of Automotive Engineering, Yancheng Institute of Technology, Yancheng, 224051, China
E-mail: sun_enhui13@163.com
DOI: https://doi.org/10.35633/inmateh-73-12

Keywords: *Stress-strain, Soil compaction, Porosity ratio, Consolidation coefficient, Orthogonal test*

ABSTRACT
In modern agriculture, with the development and widespread use of agricultural mechanization, mechanical compaction of soils has become a growing problem, resulting in soil degradation in the field. Based on the Boussinesq solution, the soil stress formula for the circular load area is derived, and MATLAB is used to simulate the stress-strain relationship of the soil at different depths. The results show that under the same load conditions, as the soil depth increases, the soil stress gradually decreases, with the most significant stress change occurring at 0.2 m depth. Soil compression experiments conducted using a consolidation instrument revealed that the soil void ratio dropped rapidly under loading of 50-200 kPa, and the decline slowed after 400 kPa. When the soil void ratio decreases to 0.2-0.4, the soil stress changes tend to stabilize. Comparison between the theoretical formula and the compression experimental data indicates that the soil stress gradually decreases as the thickness of the soil layer increases and the pressure load increases, verifying the linear relationship predicted by the theoretical formula.

摘要
在现代农业中，随着农业机械化的发展和广泛使用，土壤的机械压实已成为一个日益严重的问题，导致田间土壤退化。基于 Boussinesq 解推导了圆形荷载面积的土壤应力公式，利用 MATLAB 模拟土壤不同深度的应力-应变, 结果表明: 相同载荷条件下，土壤深度增加，土壤应力逐渐减小，在 0.2m 处应力变化最大。通过固结仪进行土壤压缩实验，结果表明：土壤孔隙比在 50-200kPa 的加载下迅速下降，在 400kPa 后下降速度减缓。当土壤孔隙比降低到 0.2-0.4，土壤的应力变化趋于稳定。通过理论公式与压缩实验数据对比结果表明：土壤应力随土层厚度增加以及压力载荷增加逐渐减小，验证理论公式的线性关系。

INTRODUCTION
Agriculture plays an important role in a country's political and economic independence (*Daneshvar et al., 2023*). With the development of agriculture, field machinery operations have become common, and people's dependence on agricultural machinery has increased. When machinery operates in the field, the traction and load of tillage machinery gradually increase, leading to greater compaction. The stress on the soil profile may exceed the soil's internal strength, resulting in changes to its physical, chemical, and biological properties, increased soil density and mechanical resistance, and reduced macropores (*Zhang et al., 2005*). This, in turn, affects crop growth in the field, as the stress from mechanical operations exceeds soil stability, leading to soil degradation.

Current research on soil stress-strain in China primarily focuses on the physical properties of soil after compaction, including factors such as soil moisture content, bulk density, porosity, and firmness that affect the internal stress-strain of soil. Based on soil stress research, soil compression tests were conducted at different depths to explore changes in soil stress-strain, providing both theoretical and experimental foundations for mitigating soil mechanical compaction.

Although agricultural machinery has been further developed, the damage to topsoil and subsoil remains significant. Soil compaction in farmland primarily results from the stress transfer within the soil under external loads, which causes soil particles to aggregate due to regular tillage compaction. This, in turn, alters the physical and chemical properties of the soil (*Naveed et al., 2016*).

[1] *Jun Guo, Ph.D. Eng.; Enhui Sun, Master; Yue Yang, Master; Jun Lu, Ph.D. Eng.*

Large agricultural machinery operations and livestock trampling generate stress transfer and shear stress in the soil, increasing the mass per unit volume and reducing soil porosity (*Carman et al., 2002*). Previous studies have shown that soil compaction from agricultural vehicles can be mitigated by reducing tire inflation pressure and increasing vehicle speed. Currently, many solutions focus on tire design, primarily by reducing the load or increasing the contact area.

Arvidsson et al., (2005), proved that tire inflation pressure significantly influences soil stress and displacement at a depth of 0.3 m. By further investigating the impact of wheel load on subsoil stress and validating the commonly used stress propagation model, they found that soil stress measured at a depth of 10 cm is highest under the greatest wheel load, indicating that both inflation pressure and wheel load affect vertical soil stress near the surface. *Lamandé et al., (2007)* studied the stress and deformation induced by loading the soil with undisturbed samples. By comparing the measured vertical stress with that calculated by the Söhne model, they found that doubling the contact area reduces stress-strain in the topsoil, with contact stress determining stress in the topsoil, while subsoil stress depends mainly on the load. *Keller et al., (2005),* developed a model in Visual Basic that predicts vertical stress distribution under a rubber track mounted on an agricultural vehicle, providing a realistic estimate of the vertical stress at the contact point of the rubber track with the soil, thereby improving the prediction of soil stress and compaction risk for rubber-tracked agricultural vehicles. *Keller et al., (2016),* used the Arvidsson probe to measure vertical stress and found, through finite element simulation, that soil properties had little effect on vertical stress. *Lamandé et al., (2018)*, analyzed the compaction effect of the same vehicle on the soil using both wheeled and crawler traveling devices and measured the distribution of vertical stress at the contact surface between the rubber crawler and the soil along the length of the crawler. Through the SoilCare project, *Piccoli et al., (2022),* studied the use of soil improvement planting systems to alleviate topsoil and internal soil compaction. Ahmed Salih Mohammed et al., (2023) used statistical modeling methods to comprehensively analyze temperature, ground granulated blast furnace slag (GGBFS) and other research parameters and evaluate their impact on the compressive strength of concrete. The experiments showed that multiple factors affect the compressive strength of soil. Through comparative experiments, *Pieniążek, (2023),* concluded that in the traditional farming system (CONV), suitable and efficient grain varieties should be selected to allow them to grow under lower fertilization conditions, so as to increase grain yield and reduce soil degradation. *Song et al., (2023)*, mixed sedimentary soil with cultivated land, compost and biochar by volume ratio to make the soil have higher water holding capacity and reduce soil loss.

Tong, (2017), determined soil strain in the contact area based on wheel movement, calculated stress for each contacting soil unit using the stress-strain relationship of vehicle-driving soil, integrated stress along the tread direction, and dynamically computed rigid ring-soil forces. *Ding, (2020),* discovered that increasing vehicle speed can reduce vertical stress in the soil, suggesting that vehicles should operate at higher speeds whenever possible to minimize soil compaction risk. *Li et al., (2010),* through actual soil tests, demonstrated that controlling soil stress within the Spc (elastic zone) effectively reduces soil compression deformation, indicating that if soil pre-consolidation pressure is lower than tire ground contact pressure, agricultural machinery operations will exacerbate soil compaction and soil structure damage. *Wang et al., (2011)*, proposed using the impact principle to detect soil compaction and established a relationship model between the impact rod and soil resistance to reflect soil compaction levels. *Song et al., (2015)*, investigated the linear relationship between resistivity and soil moisture content and compaction based on the original resistivity model of soil compaction. *He et al., (2017)*, established a linear correlation between moisture content, density, pre-consolidation pressure in the soil environment, and soil stress transfer under external force through uniaxial compression tests, aiming to predict soil compaction degree. *Wang et al., (2018),* explored the influence of soil stress on soil unit density and compaction during the transfer process of different nodes by studying tire pressure, axle load, and mechanical compaction times of agricultural machinery. They also identified the influence of soil profile stress and the number of agricultural machinery compactions using the discrete element method. *Xu, (2020),* designed a multi-directional wireless earth pressure sensor and developed a soil stress dynamic detection system for the sensor to study changes in earth pressure during soil compaction.

Considerable research has been conducted on soil compaction, resulting in a series of solutions, but most have focused on seeking remedies within agricultural machinery itself, with little emphasis on mitigating mechanical compaction from the soil itself. Currently, research on compacted soil predominantly centers on its physical and chemical properties, yielding gradual effects on alleviating soil compaction.

Assessment of soil compaction degree relies on physical quantities associated with soil compaction. Unlike the deep soil examined in soil mechanics, the soil in contact with the wheel, studied in vehicle ground mechanics, is primarily surface soil (*Zhuang, 2002*). The process of soil compaction is typically divided into three steps (*O'SullivanMF et al., 1999*): stress application to the soil surface during tire-soil interaction, stress transmission within the soil, and soil stress-induced changes in soil structure. This article focuses on the "stress transfer within the soil" process, investigating soil stress at various depths during soil compaction and identifying effective methods to alleviate soil mechanical compaction.

Building upon previous research on soil compressive stress transfer, this study addresses the limitations of existing stress transfer investigations by theoretically deducing stress transfer at various depths in the soil. Theoretical analysis of soil stress is conducted using compression test methods, with an experimental plan tailored to existing soil conditions. Soil compression tests are carried out to validate the feasibility of the soil stress theory, utilizing data obtained from the tests to examine relationships between various parameters.

MATERIALS AND METHODS

The specific research objectives are as follows:

(1) Theoretical derivation

Theoretical formulas are analyzed to establish a formula suitable for this research, and MATLAB is employed to simulate the linear relationship of the theoretical formula.

(2) Design and analysis of soil compression test

A test plan is designed in accordance with the existing soil compression test method, meeting the requirements of this study. The WG single-lever consolidation instrument (medium and low pressure) and the NSIF geotechnical test control data acquisition and processing system are utilized for the test.

Theoretical analysis

In previous stress studies, simulation and modeling methods were the primary approaches for calculating soil stress transfer. Existing analysis models all assumed that the soil is a homogeneous, elastic, and isotropic medium (*Van den Akker, 2004*). Treating the soil as an elastic-plastic material (*Smith et al., 2000*), Boussinesq deduced the stress solution at any point of the soil when the semi-infinite soil elastic body was subjected to a concentrated load in 1855 (Fig. 1).

$$\sigma_z = \frac{3Pz^3}{2\pi R^5} = \frac{3P}{2\pi R}\cos^3\theta \tag{1}$$

where P represents the concentrated load acting on the soil surface, R denotes the distance from point *M* to the center point, and θ is the angle between the R line and the vertical axis *Z*.

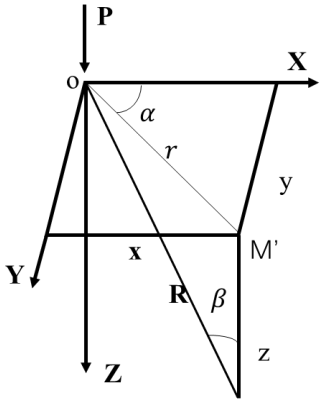

Fig. 1 - Stresses caused by concentrated loads in the vertical direction

Considering the vertical normal stress analysis in this study:

$$\sigma_z = \frac{3Pz^3}{2\pi\left(x^2+y^2+z^2\right)^{\frac{5}{2}}} = \frac{3P}{2\pi z^2}\times\frac{1}{\left[1+\left(\frac{r}{z}\right)^2\right]^{\frac{5}{2}}} = \alpha\frac{P}{z^2} \tag{2}$$

In the formula: $R^2 = r^2 + z^2$, $r^2 = x^2 + y^2$;

$\alpha = \frac{3}{2\pi} \times \frac{1}{\left[1+\left(\frac{r}{z}\right)^2\right]^{\frac{5}{2}}}$ is the stress coefficient, it is a function of *r* and *z*.

The instrument used for the soil compression experiment in this study employs a circular loading surface, so the stress under the corner point of the circular area under the action of a uniform load (Fig. 2) is:

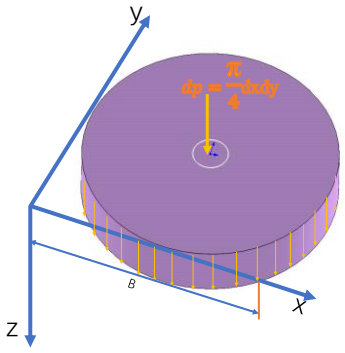

Fig. 2 - Stress under uniform circular load corner

The microelement *dxdy* is taken in the load surface, and the distributed load on the microelement is replaced by the concentrated force *dp=dxdy*, then, from the Bucinnaiske solution, it can be deduced that the point *M* at the depth *z* under the corner point *O* is subjected to the concentrated force.

The vertical stress can be obtained from the formula:

$$d\sigma_z = \frac{3z^3 p \frac{\pi}{4}}{2\pi\left(x^2+y^2+z^2\right)^{\frac{5}{2}}} dxdy = \frac{3z^3 p}{8\left(x^2+y^2+z^2\right)^{\frac{5}{2}}} dxdy \quad (3)$$

$$\sigma_z = \frac{3pz^3}{8}\int_0^1\int_0^b \frac{1}{\left(x^2+y^2+z^2\right)^{\frac{5}{2}}} dxdy = \frac{p}{8}\left[\frac{mn\left(m^2+2n^2+1\right)}{\left(m^2+n^2\right)\left(1+n^2\right)\sqrt{m^2+n^2+1}} + \arctan\frac{m}{n\sqrt{m^2+n^2+1}}\right] \quad (4)$$

In the formula: $m = \frac{l}{b}$, $n = \frac{z}{b}$, l and b are the lengths of the load acting on the farmland soil surface, respectively (*Gao, 2018*).

Simplify the above formula $\sigma_z = \alpha_c p$

$\alpha_c = \frac{1}{8}\left[\frac{mn\left(m^2+2n^2+1\right)}{\left(m^2+n^2\right)\left(1+n^2\right)\sqrt{m^2+n^2+1}} + \arctan\frac{m}{n\sqrt{m^2+n^2+1}}\right]$ *i*s the stress coefficient.

The concentration factor is influenced by both the loading environment and the soil environment. Currently, soil moisture content significantly affects the concentration coefficient, with the coefficient increasing as soil moisture content rises, according to research by *Chen et al., (2012)*. However, when moisture content is high, soil deformation after compression is substantial (*Defossez P. et al., 2003*).

Simulation of stress in the subsoil

Using the soil sample taken in this experiment as an example, the soil stress σ_z is generated by successively loading P. P ranges from 0 to 800 kPa for the test. When P ranges from 0 to 800 kPa, the distance Z between the loading point and the stress prediction point directly below is 0.02 m, 0.04 m, 0.06 m.

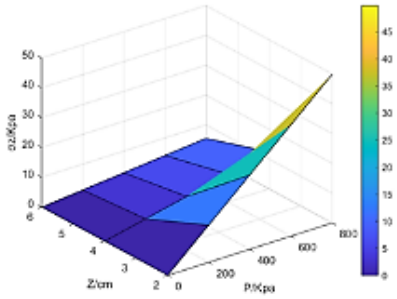

Fig. 3- σ_z Relationship between soil *P* stress and surface stress

From Fig. 3, it can be observed that using MATLAB software to analyze the theoretical formula above, there exists a relatively stable linear relationship between σ_z and P. Under the same pressure load condition, as the soil depth increases, the soil stress gradually decreases, with the most significant change occurring at 0.02 m. Under the same soil depth, soil pressure gradually increases, and the internal stress of the soil changes slowly. Due to the shallow sampling depth, the change in stress-strain is small when the loading force is low, hence the relationship between σ_z and P shown in Fig.3. When soil moisture content and wet density change, the linear relationship also remains stable.

Experimental Tests and Methods

The soil at the test site is wetland soil. Retrieved soil samples underwent rapid uniaxial compression experiments. Simultaneously, the WG-type single-lever consolidation instrument (medium and low pressure) and NSIF geotechnical tests produced by Nanjing Soil Instrument Factory Co., Ltd. were employed to control the test site. The data acquisition and processing system detected changes in the soil due to compaction, measured soil deformation and pressure, and evaluated the relationship between porosity ratio and loading pressure, as well as the consolidation coefficient and loading pressure after soil compression.

The experimental device is depicted in Fig.4, consisting mainly of the WG-type single-lever consolidation instrument (medium and low pressure), the NSIF geotechnical test control data acquisition and processing system, three dial indicators, a data collector, weights at all levels, and the test soil samples and tools.

Fig. 4 - WG type single lever consolidation instrument

The soil used in the experiment was sourced from Yancheng Institute of Technology, taken from the original soil within the 0-10 cm cultivated layer of the experimental land. Soil samples were retrieved using a ring knife with a diameter of 79.8 mm and a height of 20 mm to prepare samples located 0.02 m, 0.04 m, and 0.06 m away from the sampling ground. Each parameter's soil samples were tested multiple times, and the data were recorded (five sets of test data were analyzed for this test). A thin layer of Vaseline (*Tager et al., 2013*) was applied to the inner wall of the soil cutting ring knife used in the experiment, with the cutting edge facing downwards, and placed onto the soil sample. A soil cutter was used to cut the soil sample into soil columns slightly larger than the diameter of the ring cutter. Then, the ring knife was pressed vertically downward, and cutting proceeded while applying pressure until the soil sample protruded from the ring knife. The remaining soil at both ends was cut off and smoothed, and the outer wall of the ring knife was wiped clean. Throughout the cutting process, careful observation of the soil sample's condition was maintained. Any remaining undisturbed soil samples after cutting were wrapped in wax paper and placed in sealed bags for supplementary testing.

(1) Connect the test device, as shown in Fig.4, and place the container holding the soil sample in the pressure frame according to the test regulations, with the height of the soil sample set at 2 cm.

(2) Before commencing the test, adjust the lever to the horizontal position. To ensure optimal contact between the test soil sample and the upper and lower parts of the instrument, apply a precompression pressure of 1 kPa first according to geotechnical operating procedures. Then, adjust the dial indicator so that the pointer reads zero. Subsequently, load according to the test procedure (removing the preload weight before loading). When the soil sample sinks under pressure, causing the lever to tilt, rotate the handwheel counterclockwise to restore the lever to the horizontal position. Throughout the loading process, collect a set of data every hour until the end of pressurization.

(3) The maximum applied load for this test is 800 N. A 50 cm² soil sample container is used for the compression test. During the 50 cm² pressurization process, pressure is applied to the test soil sample through a pressure transfer plate with a diameter of 8 cm. The soil consolidation instrument is loaded step by step according to pressure levels of 50, 100, 200, 400, and 800 kPa.

(4) During the pressurization process of the test soil samples, apply the loading force to the soil samples every two loading intervals of 1 hour. After all loading levels have been applied, the test is completed once the instrument is deemed stable. Throughout the process, the NSIF geotechnical test control data acquisition system will record the vertical settlement of the pressure transfer plate and monitor the relationship between the void ratio of the ring cutter and the loading pressure, soil consolidation coefficient, and loading pressure. The ratio of pre-compressive stress to principal stress provides soil stability assessment, with values between 0.1 and 0.5 indicating weak soil conditions.

(5) Monitor soil compression by conducting compression tests on prepared soil samples using a soil consolidation instrument. Simultaneously, the NSIF geotechnical test control data acquisition and processing system will monitor and record the vertical settlement of the pressure transfer plate due to successive loading, followed by monitoring the void ratio and loading pressure of the ring cutter, and the relationship between soil consolidation coefficient and loading pressure.

(6) Analyze the changes in compressive modulus parameters, void ratio-load curve (e-p), and consolidation coefficient-load curve (cv-p) of the test soil samples based on results obtained by the NSIF geotechnical test control data acquisition and processing system.

RESULTS

Soil Compression Test Results

In Table 1 to Table 6, the vertical settlement obtained by applying the initial load is zero. Since the soil is inelastic and difficult to calculate, it is typically assumed and calculated as semi-elastic soil in actual calculations. Thus, the soil is considered a semi-infinite medium that satisfies uniform, continuous, and isotropic properties. During the experiment, the influence of the container's side wall prevents lateral deformation of the soil, which differs somewhat from the deformation of unconfined soil. However, the soil deformation observed in the test still provides valuable guidance for calculating the actual soil stress-strain distribution.

Table 1

Soil compression deformation test under lateral limit conditions 1

Pressure plate area/cm^2	Apply load / kPa	Vertical sedimentation / cm	Porosity ratio	Modulus / MPa	Compression factor / MPa^{-1}
40.24	0		0.964	0	
40.24	50	3.437	0.627	0.291	6.752
40.24	100	4.392	0.533	1.047	1.876
40.24	200	5.272	0.447	2.271	0.865
40.24	400	6.061	0.369	5.072	0.387
40.24	800	6.835	0.293	10.335	0.190

Table 2

Soil compression deformation test under lateral limit conditions 2

Pressure plate area/cm^2	Apply load / kPa	Vertical sedimenta-tion/cm	Porosity ratio	Modulus / MPa	Compression factor / MPa^{-1}
40.24	0		0.964	0	
40.24	50	4.190	0.553	0.239	8.230
40.24	100	4.923	0.481	1.364	1.440
40.24	200	5.646	0.410	2.764	0.711
40.24	400	6.326	0.343	5.884	0.334
40.24	800	6.954	0.281	12.739	0.154

Table 3

Soil compression deformation test under lateral limit conditions 3

Pressure plate area / cm^2	Apply load / kPa	Vertical sedimentation / cm	Porosity ratio	Modulus / MPa	Compression factor / MPa^{-1}
40.24	0		0.964	0	
40.24	50	4.615	0.555	0.240	8.181
40.24	100	5.086	0.465	1.086	1.809
40.24	200	5.868	0.388	2.557	0.768
40.24	400	6.571	0.319	5.692	0.345
40.24	800	7.241	0.253	11.942	0.165

Table 4

Soil compression deformation test under lateral limit conditions 4

Pressure plate area / cm^2	Apply load / kPa	Vertical sedimentation / cm	Porosity ratio	Modulus / MPa	Compression factor / MPa^{-1}
40.24	0		0.964	0	
40.24	50	3.447	0.626	0.290	6.771
40.24	100	4.692	0.504	0.803	2.446
40.24	200	5.749	0.400	1.892	1.038
40.24	400	6.613	0.315	4.626	0.425
40.24	800	7.425	0.235	9.856	0.199

Table 5

Soil compression deformation test under lateral limit conditions 5

Pressure plate area / cm^2	Apply load / kPa	Vertical sedimentation / cm	Porosity ratio	Modulus / MPa	Compression factor / MPa^{-1}
40.24	0		0.964	0	
40.24	50	2.388	0.730	0.419	4.690
40.24	100	3.508	0.620	0.892	2.201
40.24	200	4.352	0.537	2.369	0.829
40.24	400	5.044	0.469	5.783	0.340
40.24	800	5.710	0.404	12.021	0.163

Table 6

Soil compression deformation test under lateral limit conditions 6

Pressure plate area / cm^2	Apply load / kPa	Vertical sedimentation / cm	Porosity ratio	Modulus / MPa	Compression factor / MPa^{-1}
40.24	0		0.964	0	
40.24	50	4.042	0.567	0.247	7.940
40.24	100	5.378	0.567	0.247	7.940
40.24	200	6.481	0.436	0.748	2.626
40.24	400	7.387	0.328	1.814	1.083
40.24	800	8.147	0.239	4.413	0.445

Through the step-by-step loading compression experiment of the test soil, the compressive curve of the void ratio of the test soil and the external load under confinement conditions, and the variation of the compressive modulus of the test soil sample due to loading and compression were obtained. It can be observed from the following charts (Fig. 5) that as the external load increases, the soil undergoes rapid compression initially. The soil decreases rapidly during the loading process of 50-200 kPa, while the compressive modulus increases slowly during this process. Due to the gradual loading of the soil, the soil consolidation coefficient gradually decreases, indicating a slowing down of the degree of soil consolidation. The soil porosity ratio decreases slowly after loading at 400 kPa, and the compressive modulus increases rapidly after loading at 200 kPa. A larger soil void ratio corresponds to a smaller allowable bearing capacity of the soil. When the soil void ratio is reduced to 0.2-0.4, the stress-strain of the test soil tends to stabilize, further verifying the linear relationship shown by the theoretical derivation formula. The data error of the consolidation instrument range during the test can be ignored for multiple tests.

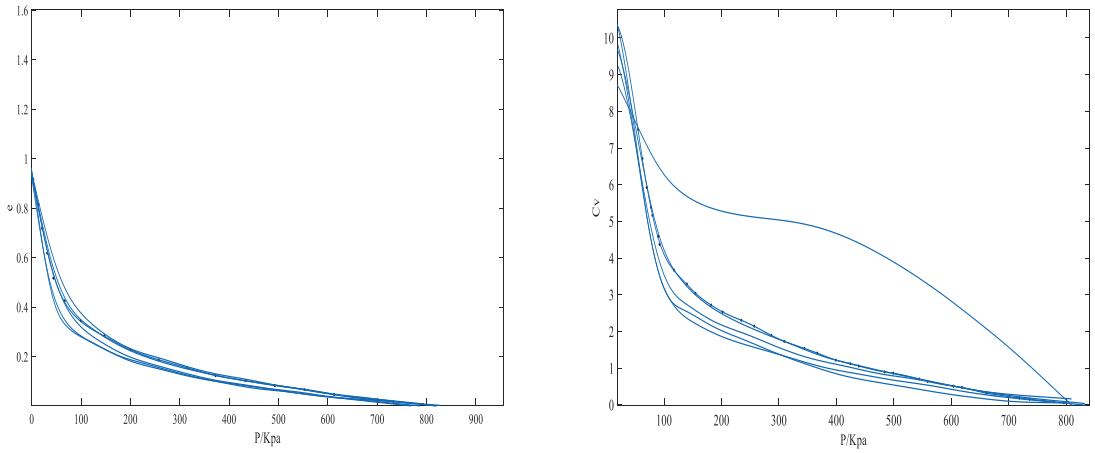

a) e-p curve b) cv-p curve

Fig. 5 - Soil compression test results

CONCLUSIONS

Based on the Boussinesq solution, the soil stress formula for the circular load area was derived, providing a theoretical basis for analyzing the stress distribution of soil under mechanical loads. Soil compression experiments were conducted, revealing that the soil void ratio decreased rapidly within a certain pressure range (50 - 200 kPa), and the decline trend slowed down after 400 kPa. Moreover, when the soil void ratio decreased to 0.2 - 0.4, the soil stress change tended to stabilize, providing experimental evidence for the compression characteristics of the soil. It helps to further understand the mechanical response and change laws of the soil under agricultural mechanization operations, providing theoretical support for reducing soil compaction, protecting soil structure and quality, and optimizing the use of agricultural machinery.

ACKNOWLEDGEMENT

This work was supported by Founding for school-level research projects of Yancheng Institute of Technology (grant 154203635), from the Yancheng Institute of Technology, of Yancheng, Jiangsu Province, China. We would like to thank Editage for providing English language editing. We are also grateful to the editor and anonymous reviewers for providing helpful suggestions to improve the quality of the present paper.

REFERENCES

[1] Carman, K., (2002), Compaction characteristics of towed wheels on clay loam in a soil bin. *Soil and Tillage Research*, 65(1), 37-43. https://doi.org/10.1016/S0167-1987(01)00281-1

[2] Chen, Z., Wang, D., Li, L., Shan R., (2012), Tensile and shear characteristics test of corn stover peel. (玉米秸秆皮拉伸和剪切特性试验), *Journal of Agricultural Engineering*, 28(21), 59-65. https://doi:10.3969/j.issn.1002-6819.2012.21.009

[3] Daneshvar, A., Radfar, R., Ghasemi, P., Bayanati, M., Pourghader Chobar, A., (2023), Design of an Optimal Robust Possibilistic Model in the Distribution Chain Network of Agricultural Products with High Perishability under Uncertainty. *Sustainability,* 15, 11669. https://doi.org/10.3390/su151511669

[4] Défossez, P., Richard, G., Boizard, H., et al., (2003), Modeling change in soil compaction due to agricultural traffic as function of soil water content. *Geoderma*, 116(1-2), 89-105. https://doi.org/10.1016/S0016-7061(03)00096-X

[5] Ding, Z., (2020), Study on soil shear and compaction process of track/wheeled combined harvester on paddy field. (履带/轮式联合收获机对稻田土壤剪切及压实作用过程研究), Jiangsu University. https://doi:10.27170/d.cnki.gjsuu.2020.000973

[6] Gao, X.Y., (2018), *Soil Mechanics*. (*土力学*), Peking University Press, Beijing, 81-85.

[7] He, T., Cong, W., Adam B E, Ding, Q., Yang, Y., Huo, L., (2017), Study on soil stress transfer coefficient based on com-paction analysis model. (基于压实分析模型的土壤应力传递系数研究), *Transactions of the CSAM*, 48(06), 59-65. https://doi: 10.6041/j.issn.1000-1298.2017.06.007

[8] Lamandé, M., Greve, M.H., Schjønning, P., (2018), Risk assessment of soil compaction in Europe-Rubber tracks or wheels on machinery. *Catena*, 167(41), 353-362. https://doi.org/10.1016/j.catena.2018.05.015

[9] LI, C., Ding, Q., Chen, Q., (2010), Determination and analysis of advanced consolidation pressure in paddy soil. (水稻土的先期固结压力测定与分析), *Transactions of the Chinese Society of Agricultural Engineering*, 26(08), 141-144. https://doi: 10.3969/j.issn.1002-6819.2010.08.024

[10] Lamandé, M., Schjønning, P., Tøgersen, F.A., (2007), Mechanical behaviour of an undisturbed soil subjected to loadings: Effects of load and contact area. *Soil and Tillage Research*, 91-106. https://doi.org/10.1016/j.still.2007.09.002

[11] Mohammed, A.K., Hassan, A.M.T., Mohammed, A.S., (2023), Predicting the Compressive Strength of Green Concrete at Various Temperature Ranges Using Different Soft Computing Techniques. *Sustainability*, 15, 11907. https://doi.org/10.3390/su151511907

[12] Naveed, M., Schjønning, P., Keller, T., et al., (2016), Quantifying vertical stress transmission and compaction-induced soil structure using sensor mat and X-ray computed tomography. *Soil and Tillage Research*, 158. https://doi.org/10.1016/j.still.2015.12.006

[13] O'Sullivan, M.F., Henshall, J.K., Dickson, J.W., (1999), A simplified method for estimating soil compaction. *Soil and Tillage Research*, 49(4), 325-335. https://doi.org/10.1016/S0167-1987(98)00187-1

[14] Piccoli, I., Seehusen, T., Bussell, J., Vizitu, O., Calciu, I., Berti, A., Börjesson, G., Kirchmann, H., Kätterer, T., Sartori, F., et al., (2022), Opportunities for Mitigating Soil Compaction in Europe—Case Studies from the SoilCare Project Using Soil-Improving Cropping Systems. *Land*, 11(2). https://doi.org/10.3390/land11020223

[15] Pieniążek, J.M., (2023), The Influence of Cropping Systems on Photosynthesis, Yield, and Grain Quality of Selected Winter Triticale Cultivars. *Sustainability*, 15, 11075. https://doi.org/10.3390/su151411075

[16] Smith, R., Ellies, A., Horn, R., (2000), Modified Boussinesq's equations for nonuniform tire loading. *Journal of Terramechanics*, 37(4), 207-222. https://doi.org/10.1016/S0022-4898(00)00007-0

[17] Song, J., LI, S.C., Liu, B., Xu, X., Wang, C., Nie, L., (2015), Quantitative evaluation method of compaction degree of unsaturated soil based on resistivity characteristics, (基于电阻率特性的非饱和土

压实度定量评价方法). *Journal of Chang'an University (Natural Science Edition)*, 35(06, 33-41. https://doi: JournalArticle/5b3c22e1c095d70f00a9c1aa

[18] Song, Y., Kim, S.; Koo, H., Kim, H., Kim, K., Lee, J., Jang, S., Lee, K.C., (2023), Assessing the Suitability of Sediment Soil to Be Reused by Different Soil Treatments for Forest Agriculture. *Sustainability*, 15, 11477. https://doi.org/10.3390/su151511477

[19] Tagar, A.A., Ji, C., Ding, Q., et al., (2014), Soil failure patterns and draft as influenced by consistency limits: an evaluation of the remolded soil cutting test. *Soil and Tillage Research*, 137, 58-66. https://doi.org/10.1016/j.still.2013.12.001

[20] Keller, T., Arvidsson, J., (2016), A model for prediction of vertical stress distribution near the soil surface below rubber-tracked undercarriage systems fitted on agricultural vehicles. *Soil and Tillage Research*, 116-124. https://doi.org/10.1016/j.still.2015.07.014

[21] Keller, T., (2005), A Model for the Prediction of the Contact Area and the Distribution of Vertical Stress below Agricultural Tyres from Readily Available Tyre Parameters. *Biosystems Engineering*, 85-96. https://doi.org/10.1016/j.biosystemseng.2005.05.012

[22] Keller, T., Ruiz, S., Stettler, M., Berli, M., (2016), Determining Soil Stress beneath a Tire: Measurements and Simulations. Soil Science Society of America Journal, 80: 541-553. https://doi.org/10.2136/sssaj2015.07.0252

[23] Tong, K., (2017), Study on dynamic contact force model of tire-soft road surface. (轮胎-松软路面动态接触力模型研究). Jilin University. https://doi:CNKI:CDMD:2.1017.156238

[24] Van den Akker, Jan J.H., (2004), SOCOMO: a soil compaction model to calculate soil stresses and the subsoil carrying capacity. *Soil and Tillage Research*, 79(1), 113-127. https://doi.org/10.1016/j.still.2004.03.021

[25] Wang, J.F., Chen, X.X., (2011), Application of impact principle in soil compaction measurement technology. (冲击原理在土壤压实测量技术中的应用). *Agricultural Equipment and Vehicle Engineering*, (02), 49-51. https://doi:10.3969/j.issn.1673-3142.2011.02.016

[26] Wang, X.L., (2018), Research on soil compaction evaluation and combined shoveling and ripping technology of agricultural machinery. (农机作业土壤压实评价及组合铲松土技术研究). China Agricultural University.

[27] Xu, J.X., (2020), Research on multi-directional wireless soil pressure sensor and monitoring system in farmland. (农田多向无线土压力传感器及监测系统的研究). Northeast Agricultural University. https://doi: 10.27010/d.cnki.gdbnu.2020.000953

[28] Zhang, X.Y., Sui Y.Y., (2005), Research progress of mechanical soil compaction in farmland. (农田土壤机械压实研究进展). *Transactions of the CSAM*, 36(6), 122-125. https://doi:10.3969/j.issn.1000-1298.2005.06.033

[29] Zhuang, J.D., (2002), *Calculation of automobile ground mechanics*. (*计算汽车地面力学*). Beijing: China Machine Press, Beijing.